

# Chemical Bath Deposition of Bismuth Oxide (Bi<sub>2</sub>O<sub>3</sub>) Thin Film and its Applications

F.I. Ezema, Ph.D. and C.E. Okeke, Ph.D.

Department of Physics and Astronomy, University of Nigeria

Nsukka, Enugu State, Nigeria

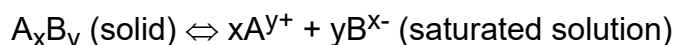
## ABSTRACT

Bismuth oxide (Bi<sub>2</sub>O<sub>3</sub>) thin films on glass slides were prepared using chemical bath deposition techniques and were characterized using energy dispersive x-ray fluorescence (EDXRF), Fourier transforms infrared (FTIR) spectroscopy, and spectrophotometers. Film thickness in the range between 0.089 and 0.099 μm with energy band gap between 2.50 and 3.60eV have been deposited. The data from spectrophotometric analysis showed that average n values range between 1.31 and 1.38, k ranges are between 1.63 x 10<sup>-3</sup> and 2.22 x 10<sup>-3</sup>, and σ<sub>o</sub> ranges are between 0.012 x 10<sup>14</sup>S<sup>-1</sup> and 0.019 x 10<sup>14</sup>S<sup>-1</sup>. The films are good transmitters of radiation; in the UV-VIS-NIR spectra range between 82 and 100%, while in the far infrared regions it ranges between 15 and 59%. The films show poor absorbance in the UV-VIS-NIR regions; hence they have potential applications in thermal control coatings for cold climates and antireflection coatings.

(Key words: chemical bath deposition, bismuth oxide)

## INTRODUCTION

The chemical bath deposition technique has been referred to as autocatalytic deposition, electroless deposition, or the solution growth technique. This technique is employed in depositing conducting and non-conducting thin films from chemical bath solutions by electrochemical processes without the presence of an externally applied field [1]. Both metallic and non-metallic ions, which are present in the chemical bath deposition, react with each other and become neutral atoms, which either precipitate spontaneously or deposit very slowly in the bath. Spontaneous precipitation implies that films will not be deposited on a substrate; hence appropriate complexing agents slow the reaction down so that thin solid films of neutral atoms could form on a substrate without application of an external field. When the ionic product (I.P.) of compounds which are slightly soluble in a solvent exceed their solubility product (S.P.) constant, K<sub>sp</sub> the compounds can be precipitated from their solution (i.e. I.P. > S.P.). For example, in a saturated solution, an ionic compound A<sub>x</sub>B<sub>y</sub> dissociates according to the equation:



$$\text{I.P.} = [A^{y+}]^x [B^{x-}]^y$$

where  $[A^{y+}]$  and  $[B^{x-}]$  are molar concentrations of the ions  $A^{y+}$  and  $B^{x-}$  respectively,  $K_{sp}$  for compounds at particular temperatures are obtained from standard tables [2]. At equilibrium,  $I.P = K_{sp}$  at constant temperature, so in knowing both  $K_{sp}$  for  $A_xB_y$  and the molar concentration of the ions in solution, the unknown molar concentration needed to make  $I.P. > S.P.$  can be computed.

In the case of oxide films, the deposition follows in two steps, which includes the deposition of a hydrous film and its pyrolytic decomposition into the anhydrous film [3]. The deposition of the film begins with nucleation phase, then proceeds through a growth phase in which the film's thickness increases via ion-by-ion condensation [4], which rules out the issue of precipitation. The growth phase consists of a slowed down (controlled) reaction, where a complexing agent slowly releases the free ions according to the equilibrium reaction of the form:



where  $m^{z+}$  is the metal ion and A is the complexing agent. The negative ions necessary for the compound film formation can also be generated slowly by means of suitable complexing agents bearing the ions.

This technique has become part of a new, intensively studied thin film deposition method for synthesis of various functional coatings [5-14], which are mostly sulphide thin films and in particular cadmium sulphide. They are being used to develop thin films for photothermal and photovoltaic conversions, decorative and protective coatings, and imaging techniques [11-13]. Solar and ultrasonication assisted chemical bath deposition have also been reported [3, 6,14].

## THEORETICAL CONSIDERATION and CALCULATIONS

In both crystalline and amorphous semiconductors, near the fundamental absorption age there is the dependence of the absorption coefficient on the photon energy. In high absorption region, the form of absorption coefficient with photon energy was given in a more general term by [15] as:

$$\alpha = A (\alpha h\nu - E_g)^n \dots\dots\dots 1$$

where  $\nu$  is the angular frequency of the incident photon,  $h$  is plank's constant,  $A$  is a constant,  $E_g$  is the optical energy gap, and  $n$  is the number which characterizes the optical processes. Variable  $n$  has the value  $1/2$  for direct allowed transition, and has the value  $2$  for indirect allowed transition. When the straight portion of the  $\alpha^2$  against  $h\nu$  is extrapolated to  $\alpha^2 = 0$ , this gives the direct energy band gap of the material. For semiconductors and insulators (where  $k^2 \ll n^2$ ), there exist a relationship between  $R$  and  $n$  given by [16]:

$$R = (n-1)^2 / (n+1)^2 \dots\dots\dots 2$$

There is also a relationship between  $k$  and  $\alpha$  given by [15]:

$$K = \alpha \lambda / 4\pi \dots\dots\dots 3$$

where  $\alpha$  = absorption coefficient of the film and  $\lambda$  = wavelength of electromagnetic wave. The relationship between  $\varepsilon$  and  $k$  is given by [15]:

$$\varepsilon = \varepsilon_r + \varepsilon_i = (n + ik)^2 \dots\dots\dots 4$$

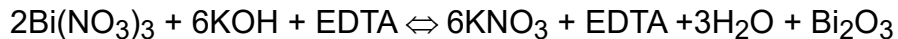
where  $\varepsilon_r$  and  $\varepsilon_i$  are real and imaginary parts of  $\varepsilon$  respectively. Optical conductivity  $\sigma$  is given by [15]:

$$\sigma = \alpha nc/4\pi \dots\dots\dots 5$$

where  $c$  is the velocity of light. Optical methods as discussed by Theye [17] and Ezema [18] were used to estimate the thickness of the film.

The deposition of the bismuth oxide thin film was done using a chemical bath that consist of bismuth nitrate, potassium hydroxide (KOH), ethylene diamine tetra acetic acid (EDTA), and distilled water. A chemical bath deposition technique was employed in the deposition of bismuth oxide (Bi<sub>2</sub>O<sub>3</sub>) films on glass slides at room temperature. The substrates were previously degreased in hydrochloric acid and nitric acid for 48 hours, cleaned with detergent in cold water, rinsed with distilled water, and allowed to drip dry in air. To produce Bi<sub>2</sub>O<sub>3</sub> thin films, an alkaline solution of bismuth salt, EDTA, and KOH was prepared. The reaction baths for the deposition contain solutions of EDTA complex of bismuth and potassium hydroxide in cold water. The reaction baths were made up of given volumes of Bi(NO<sub>3</sub>)<sub>3</sub> 5H<sub>2</sub>O, EDTA, and KOH solutions added into 50ml beakers in that order, which were stirred thoroughly using glass rods at each stage to obtain a homogenous mixture of the solutions. Some reaction baths contained KOH without EDTA, while some contain EDTA without KOH. Each bath was brought to 40ml volume with distilled water and allowed to stay for 22 and 24 hours dip times. The reaction baths were tested for their pH value (alkaline medium) before the substrates were introduced in the solutions. The reaction was a hydrolysis reaction [19], occurring at room temperature with EDTA and/or KOH acting as complexing agent in alkaline medium.

The basic reaction involved is stated below:



The EDTA and/or KOH acts as a complexing agent in the reaction. Table 1 shows the various iterations of reaction baths and dip times.

**Table 1.** The Preparation of Bismuth Oxide.

Reaction Bath	Dip. Time	Bi(NO <sub>3</sub> ) <sub>3</sub> 5H <sub>2</sub> O	EDTA	KOH	H <sub>2</sub> O	

	(hr)	Mol. (m)	Vol. (ml)	Mol. (m)	Vol. (ml)	Mol. (m)	Vol. (ml)	Vol. (ml)	pH
B <sub>1</sub>	22	0.1	5	0.1	2	1.0	10	23	12.8
B <sub>3</sub>	22	0.1	5	0.1	2	1.0	10	23	8.21
B <sub>4</sub>	22	0.1	5	0.1	2	0.5	4	29	9.60
BO <sub>1</sub>	24	0.1	5	-	-	1.0	10	25	12.0
BO <sub>2</sub>	24	0.1	5	-	-	1.0	10	25	12.5

After the films were deposited, they were rinsed in distilled water and allowed drip dry in air. The films were then characterized using EDXRF, FTIR spectroscopy, and spectrophotometers. The spectral absorbance/transmittance characteristics of the film were obtained using PYE UNICAM UV SP8-100 spectrophotometers in the UV-VIS-NIR regions while FTIR spectrometer were used in the far infrared regions. The optical properties studied include the Absorbance (A), Transmittance (T) and Reflectance(R), which were used to calculate the other properties such as refractive index (n), extinction coefficient (k), dielectric constant ( $\epsilon$ ) and optical conductivity ( $\sigma$ ).

## RESULTS AND DISCUSSION

The EDXRE show that Bismuth peak was recorded at 10.83keV. The blank background of infrared spectroscopy for nujol (Figure 1) indicates peaks at  $1377\text{cm}^{-1}$ ,  $1461\text{cm}^{-1}$ ,  $2855\text{cm}^{-1}$ ,  $2924\text{cm}^{-1}$ ,  $2953\text{cm}^{-1}$  and  $3436\text{cm}^{-1}$  with percentage transmittance between 5 - 57%. When the film was dissolved in nujol (Figure 2), it showed peaks at  $1326$ ,  $1118$ ,  $1031\text{cm}^{-1}$ ,  $876\text{cm}^{-1}$ ,  $655\text{cm}^{-1}$  and  $540\text{cm}^{-1}$  with transmittance between 62 and 72%, resulting from the dissolved film. However, the new nujol peaks show transmittance ranging between 46 and 63%. The transmittance of the film with regard to nujol peaks, before dissolving the film, and new nujol peaks after dissolving the film, show that transmittance ranged between 15 and 59%. Comparing the nujol spectra to spectra recorded after dissolving of the film in the nujol, the percentage transmittance after dissolving of the film is higher than that before dissolving of the film.

**Figure 1.** Spectral Infrared Transmittance for Nujol.

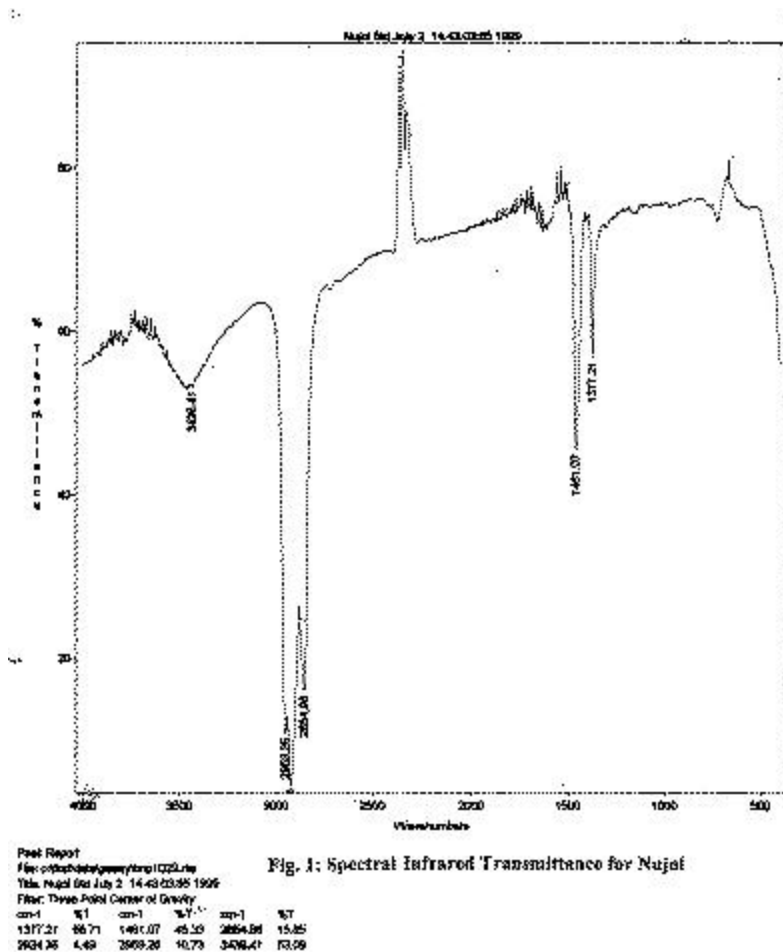


Fig. 1: Spectral Infrared Transmittance for Nujol

This means that the film enhances transmittance within the far infrared regions. Nitrogen from bismuth nitrate has the following absorption bands;  $\text{NO}_2^-$  has absorption band between  $1385\text{-}1323\text{ cm}^{-1}$ ,  $1262\text{ - }1231\text{ cm}^{-1}$  and  $862\text{ - }815\text{ cm}^{-1}$  while  $\text{NO}_3^-$  has between  $1400\text{-}1354\text{ cm}^{-1}$  and  $869\text{-}808\text{ cm}^{-1}$  [20]. The peak recorded at  $1326\text{ cm}^{-1}$  could be attributed to O - H bonds [21] and/or an incorporation of nitrogen from bismuth nitrate into the films as reported [20] for its compound  $\text{NO}_2^-$  in the range  $1323\text{ -}1339\text{ cm}^{-1}$ , as can be seen from Figure 2.

Figure 2. Spectral Infrared Transmittance of Combined Film-Nujol System.

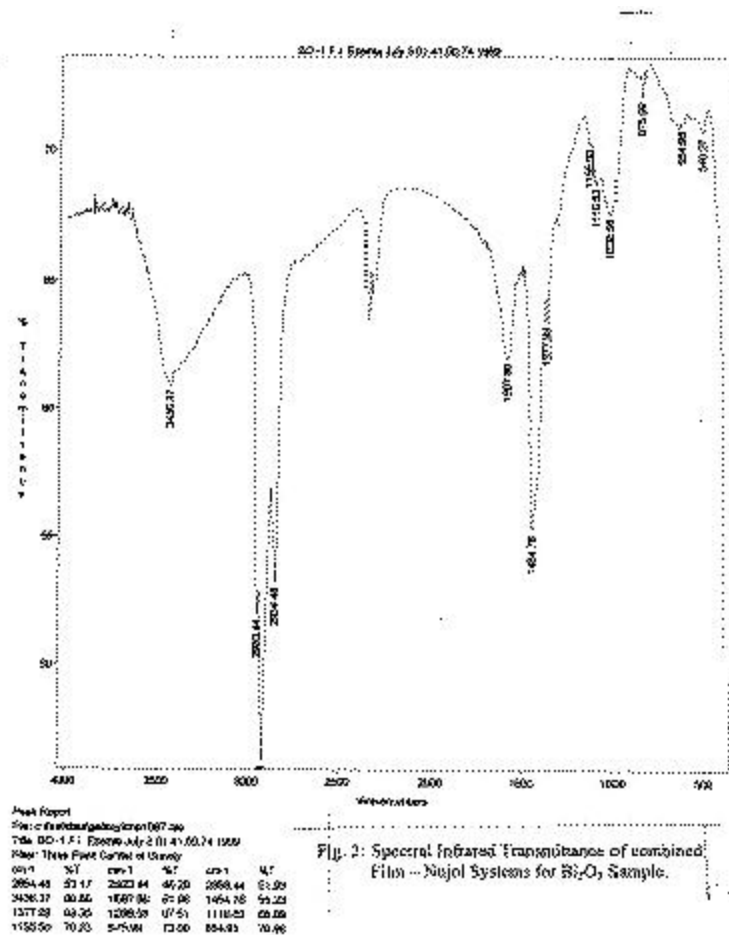


Fig. 2: Spectral Infrared Transmittance of combined Film-glass Systems for  $\text{Bi}_2\text{O}_3$  Sample.

However, the absence of the peaks from water of crystallization in the films confirms the films to be oxide with impurities, due to the incorporated nitrogen from  $\text{NO}_2^-$  (from the bismuth nitrate).

Figures 3 and 4 show the combined effect of the film-glass system on transmittance of infrared radiation for  $\text{Bi}_2\text{O}_3$  when compared with uncoated glass. This experiment was carried out using a single beam Fourier transform spectrometer. Uncoated glass (Figure 3) reduced transmittance to 33.99% at  $3462\text{cm}^{-1}$ ; then to 34.09% at  $2857\text{cm}^{-1}$ ; and finally to only about 2% transmittance in the  $1896\text{cm}^{-1}$  to  $2000\text{cm}^{-1}$  range. At around  $2001\text{cm}^{-1}$ , no radiation is transmitted through the glass.

Figure 3. Spectral Infrared Transmittance of Plain Glass.

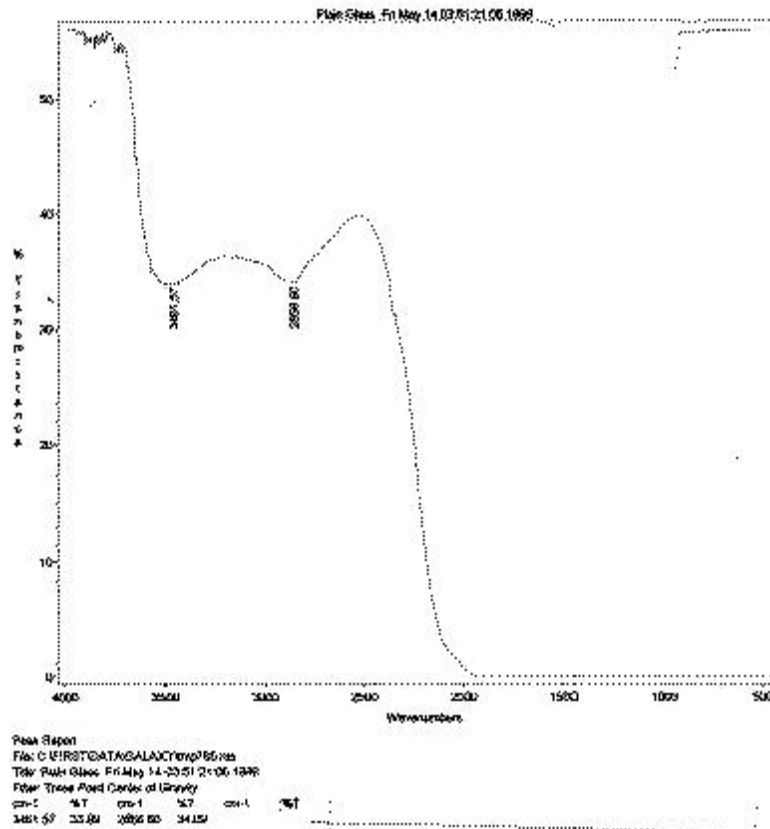
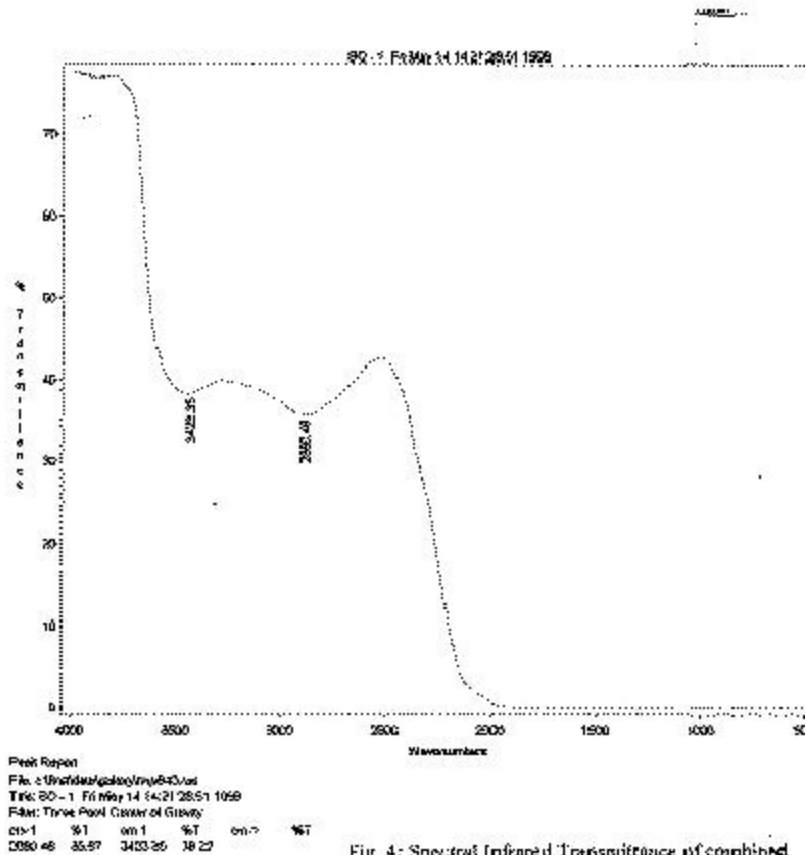


Fig. 3: Spectral Infrared Transmittance of Plain Glass

Using coated glass with the film (Figure 4) reduced transmittance to 38.22% at  $3423\text{cm}^{-1}$ , then 35.67% at  $2881\text{cm}^{-1}$ , and 2% transmittance at  $1896\text{cm}^{-1} - 2000\text{cm}^{-1}$ . By about  $2001\text{cm}^{-1}$ , no radiation is transmitted through the film-glass system.

**Figure 4.** Spectral Infrared Transmittance of Combined Film-Glass System.



These films are capable of allowing solar radiation (0.3 - 3.0 $\mu$ m) to be transmitted into a building, but preventing thermal re-radiation out of the building through the glassing system. It is observed that the film-glass system enhances transmittance of IR more than plain glass, just as the film-nujol system enhances transmittance of IR more than plain nujol. The spectral absorbance of bismuth oxide film prepared at 300k is displayed in Figure 5.

**Figure 5.**



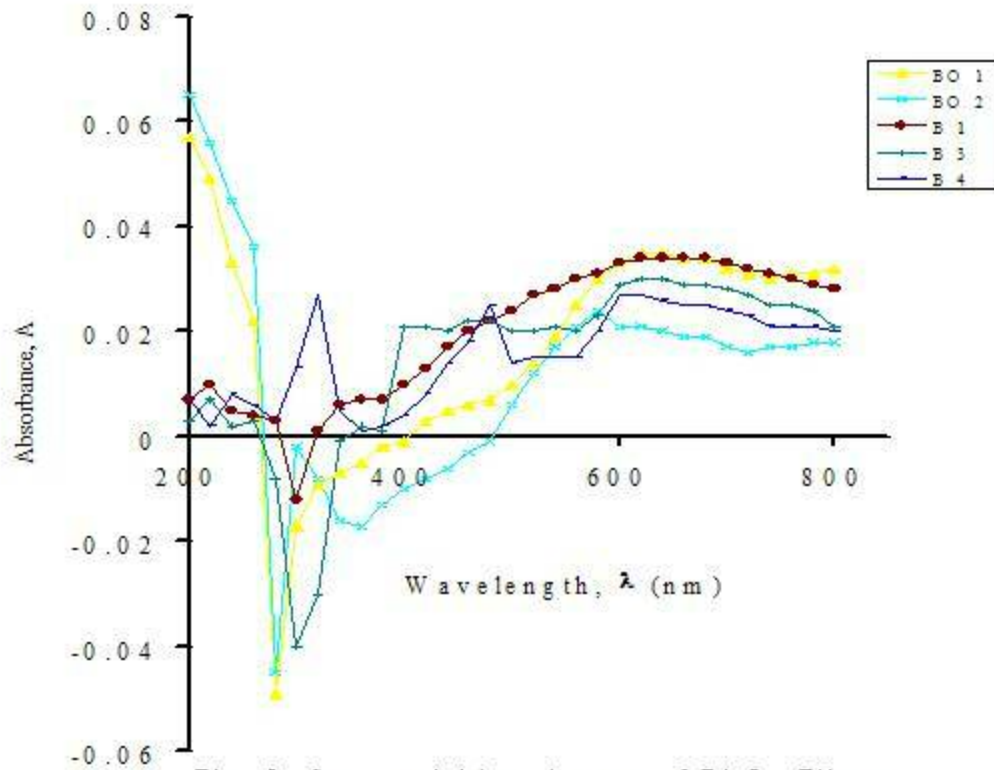


Fig. 5: Spectral Absorbance of  $\text{Bi}_2\text{O}_3$  Films Prepared at 300k.

Samples of  $\text{BO}_1$  and  $\text{BO}_2$  show negative minimum absorbance at  $\lambda$  of 280nm with absorbance of - 0.049 and - 0.045 respectively.  $\text{B}_1$  and  $\text{B}_2$  observed their own negative minimum absorbance at 300nm with absorbance of - 0.012 and - 0.040 respectively. The phenomenon of negative absorbance could indicate that the films are emitting light and at the same time absorbing radiation. These emissions reinforce the incident radiation at the fundamental absorption region. This makes it appear as if the transmitted light is greater than the incident light [22]. The negative absorbance behavior could be attributed to thermoluminescence(TL), photoluminescence(PL) or electroluminescence(EL) properties of bismuth oxide films. The phenomenon of negative absorbance of films were expressed in the work of Ndukwe [23].

All the samples of the films produced in this study exhibit poor absorbance through all UV-VIS-NIR regions. The transmittance - reflectance spectra are displayed in Figures 6 and 7.

Figure 6.

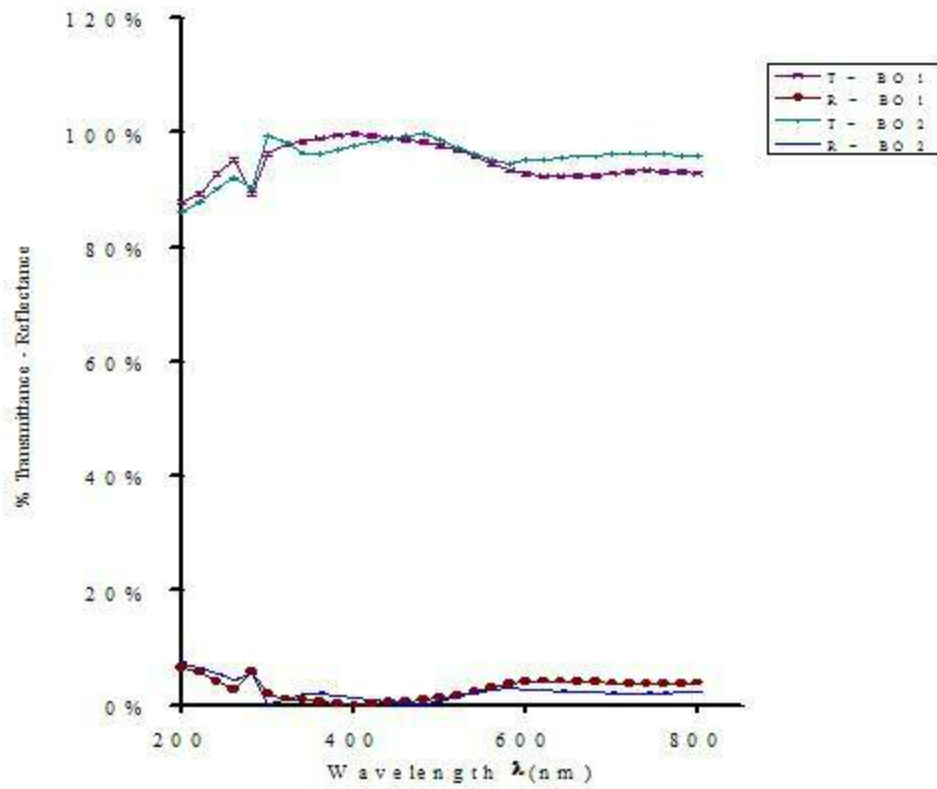


Fig. 6: Spectral Transmittance - Reflectance for  $\text{Bi}_2\text{O}_3$  Films prepared at 300k.

Figure 7.

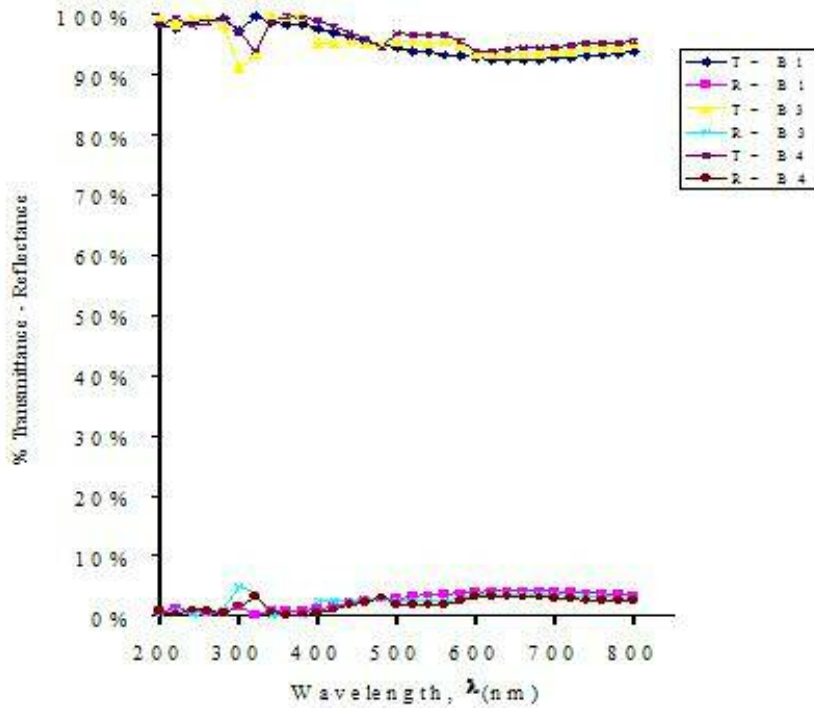


Fig. 7: Spectral Transmittance - Reflectance of  $\text{Bi}_2\text{O}_3$  Film prepared at 300k.

All of the films exhibit high transmittance throughout UV-VIS-NIR regions while exhibiting low reflectance the same regions. The properties of high transmittance throughout the UV-VIS-NIR range makes the films good materials for thermal control window coatings for cold climates and antireflection coatings. The variation of  $n$  and  $k$  with  $h\nu$  for sample of  $\text{Bi}_2\text{O}_3$  are shown in Figure 8.

**Figure 8.**

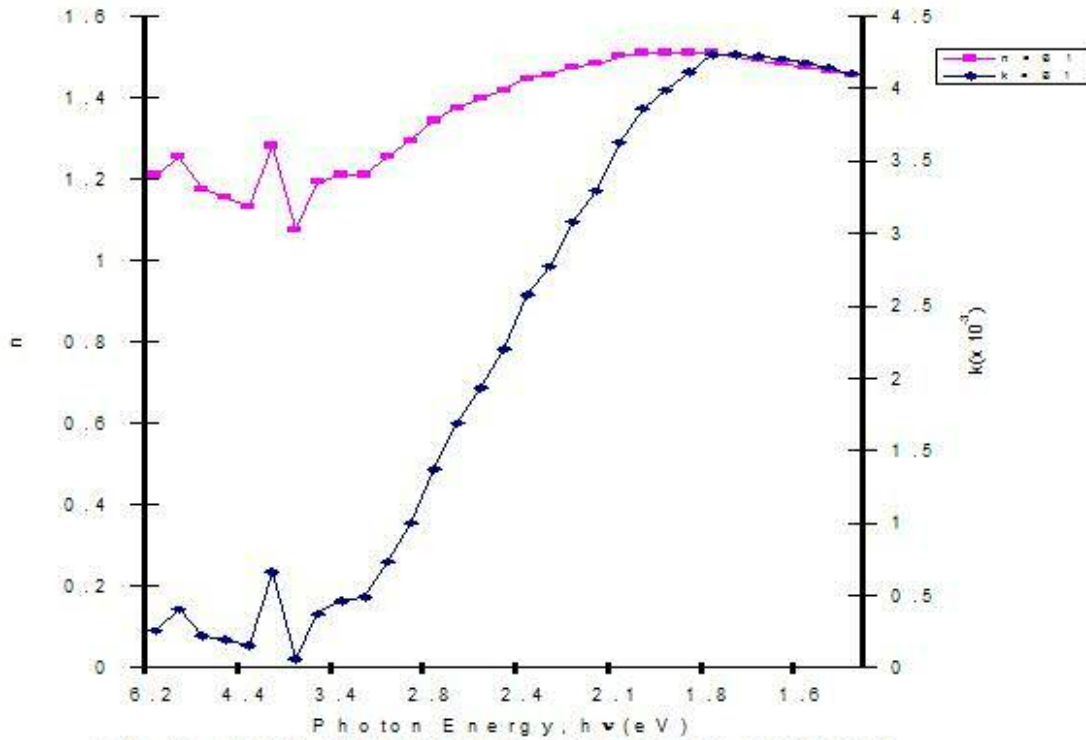


Fig. 8: Plots of Refractive Index  $n$  and Extinction Coefficient  $k$  against  $h\nu$  for  $\text{Bi}_2\text{O}_3$  Sample.

It is observed that  $n$  and  $k$  reached maximum values of 1.51 and  $4.235 \times 10^{-3}$  at 1.83eV and decreased to minimum values of 1.08 and  $0.059 \times 10^{-3}$  at 3.88eV. This is in agreement with the findings of Greenaway and Harbeke [24], which stated that for semiconductors, it is expected that the maximum in the refractive index ( $n$ ) will occur at the energy near that at which the maximum change in  $k$  occurs.

The plot of optical conductivity  $\sigma_o$  against  $h\nu$  is shown in Figure 9. It has a maximum value of  $0.028 \times 10^{14}\text{S}^{-1}$  at 1.83eV and a minimum value of  $0.0006 \times 10^{14}\text{S}^{-1}$  at 3.88eV. Table 2 shows the summary of the average optical properties and thickness of  $\text{Bi}_2\text{O}_3$  films prepared at 300k.

**Figure 9.**

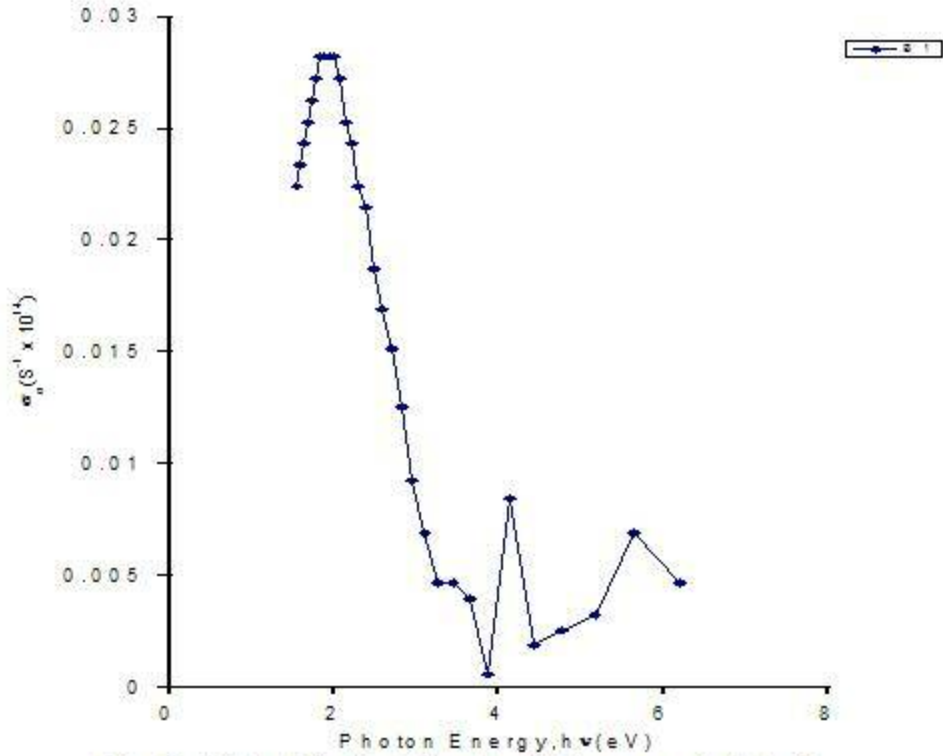


Fig. 9: Plot of Optical Conductivity  $\sigma_o$  against  $h\nu$  for  $Bi_2O_3$  Sample.

**Table 2.** Average Optical Properties and Thickness of  $Bi_2O_3$  Films.

Sample No	Dep. Time (hr)	pH	Avg. $\alpha$ $\times 10^6 m^{-2}$	Avg. N	Avg. $k \times 10^{-3}$	Avg. $\sigma_o$ $10^{14} S^{-1}$	Avg. $t$ ( $\mu m$ )
B <sub>1</sub>	22	12.8	0.0472	1.363	2.2190	0.0162	0.096
B <sub>3</sub>	22	8.21	0.0449	1.351	1.9957	0.0152	0.092
B <sub>4</sub>	22	9.60	0.0358	1.310	1.6315	0.0117	0.089
BO <sub>1</sub>	24	12.0	0.0541	1.387	2.2221	0.0193	0.099
BO <sub>2</sub>	24	12.5	0.0456	1.352	1.6245	0.0159	0.093

Although there is no established correlation between the thickness and pH, the most favorable conditions for the deposition of the film has been demonstrated [19] to be in an

alkaline medium. The maximum and minimum of thickness of  $0.099\mu\text{m}$  and  $0.089\mu\text{m}$  occurred at average maximum and minimum absorption coefficient corresponding to  $0.0541 \times 10^6\text{m}^{-2}$  and  $0.0358 \times 10^6\text{m}^{-2}$  respectively. The absorbance of the film depends on the thickness of the film [19], hence the absorbance increased as thickness increased, as expected.

The plots of  $\epsilon_r$  and  $\epsilon_i$  against  $h\nu$  are displayed in Figure 10. It can be seen that the shapes of the spectral curves for  $n$  and  $k$  (Figure 8) and of  $\epsilon_r$  and  $\epsilon_i$  are strikingly similar.

**Figure 10.**

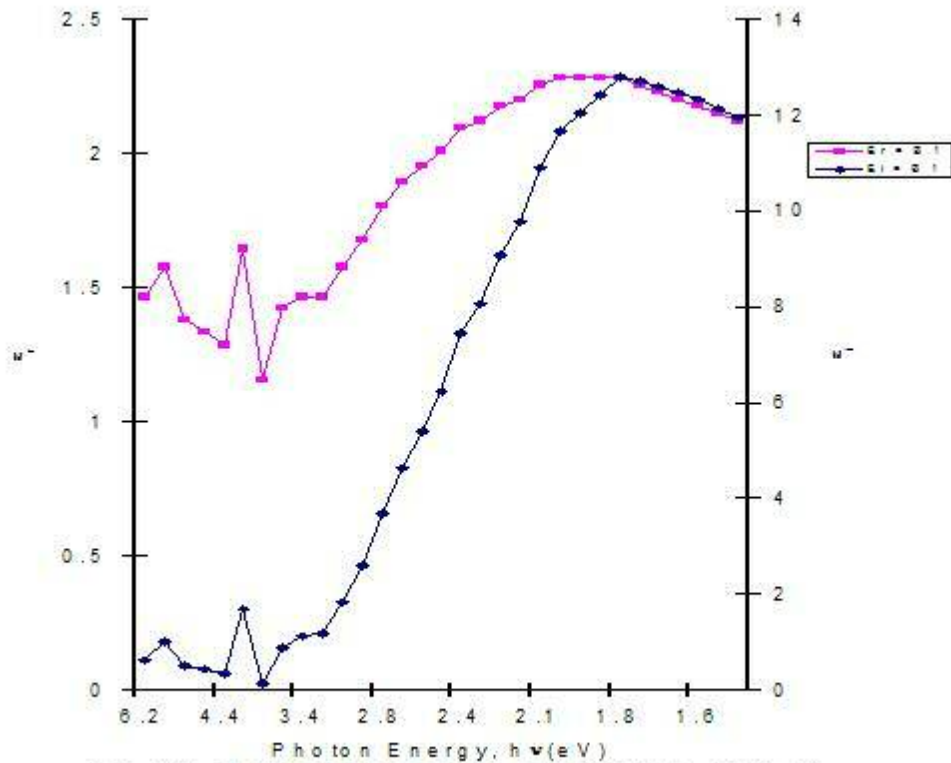


Fig. 10: Plots of Real  $\epsilon_r$  and Imaginary  $\epsilon_i$ , parts of Dielectric Constant against  $h\nu$  for  $\text{Bi}_2\text{O}_3$  Sample.

$\epsilon_r$  has a minimum value of 0.126 at 3.88eV and a maximum value of 2.28 at 1.83eV while  $\epsilon_i$  has minimum value of  $1.55 \times 10^{-3}$  3.88eV and a maximum value of  $12.790 \times 10^{-3}$  at 1.83eV. All the values for complex refractive index, dielectric constant and optical conductivity decrease from the maximum values at low energy regions to minimum values at the higher energy regions. The optical absorption coefficient  $\alpha$  against  $h\nu$  is shown in Figure 11.

**Figure 11.**

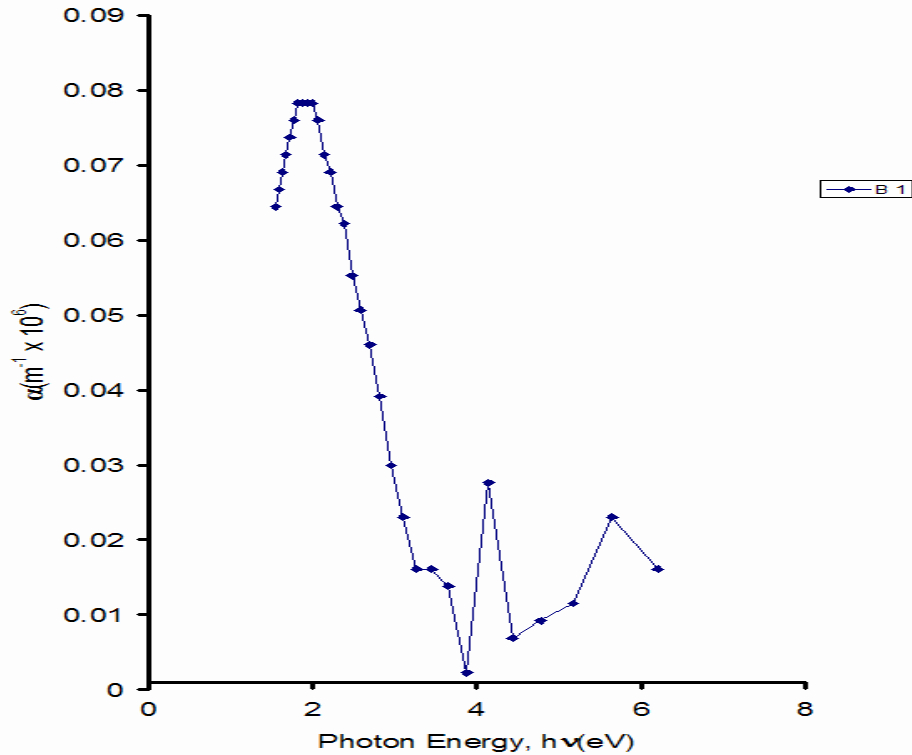


Fig. 11: Plot of Absorption Coefficient  $\alpha$  against  $h\nu$  for  $\text{Bi}_2\text{O}_3$  Sample.

This curve shows a maximum value of  $0.078 \times 10^6 \text{ m}^{-1}$  at  $1.83 \text{ eV}$  and a minimum value of  $0.0023 \times 10^6 \text{ m}^{-1}$  at  $3.88 \text{ eV}$ . The plots of  $\alpha^2$  against  $h\nu$  for  $\text{Bi}_2\text{O}_3$  films are shown in Figures 12 and 13. These reveals band gap range between  $2.50$  and  $3.60 \text{ eV}$  with optimum value of  $3.60 \text{ eV}$ . Table 3 shows the summary of the average solid-state properties and thickness.

Figure 12.

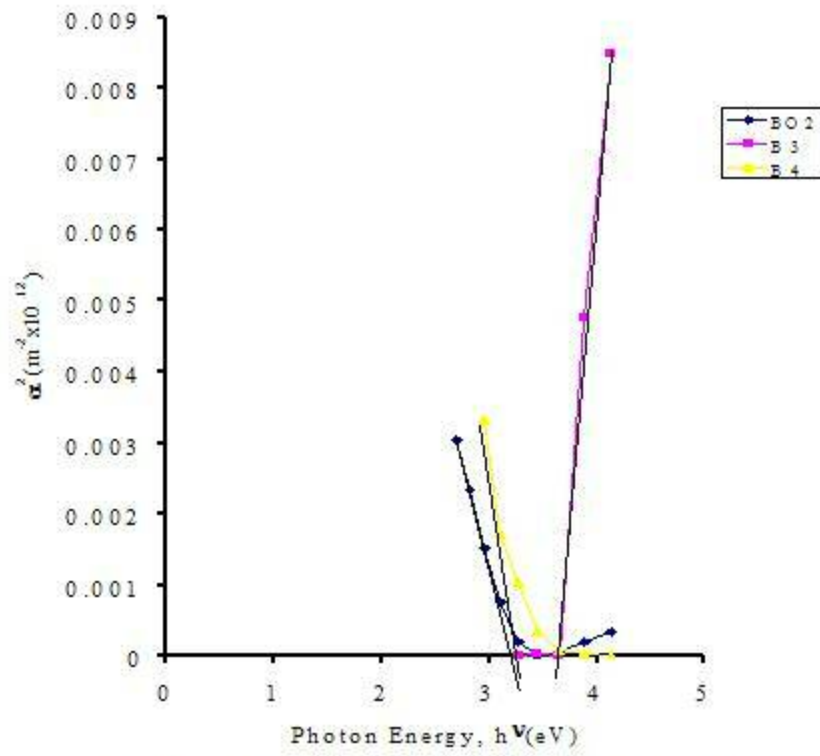


Fig. 12: Plots of  $\alpha^2$  against  $h\nu$  for  $Bi_2O_3$  Samples.

Figure 13.



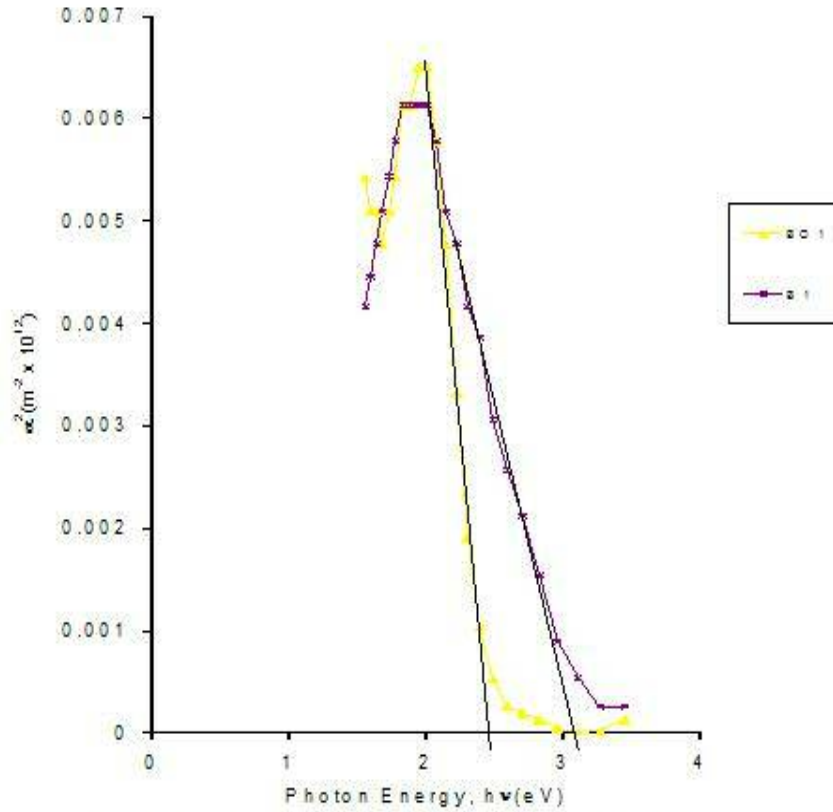


Fig. 13: Plots of  $\alpha^2$  against  $h\nu$  for  $\text{Bi}_2\text{O}_3$  Samples.

**Table 3.** Average Solid-State Properties and Thickness for  $\text{Bi}_2\text{O}_3$  Films.

Sample No	Dep. Time (hr)	pH	Avg. $\alpha$ $\times 10^6 \text{m}^{-2}$	Band Gap (eV)	Avg. $\epsilon_r$	Avg. $\epsilon_i$ ( $\times 10^{-3}$ )	$t$ ( $\mu\text{m}$ )
B <sub>1</sub>	22	12.8	0.0472	3.10	1.876	6.4714	0.096
B <sub>3</sub>	22	8.21	0.0449	3.60	1.843	5.6969	0.092
B <sub>4</sub>	22	9.60	0.0358	3.34	1.730	4.5195	0.089
BO <sub>1</sub>	24	12.0	0.0541	2.50	1.952	6.5752	0.099
BO <sub>2</sub>	24	12.5	0.0456	3.27	1.851	4.5743	0.093

## CONCLUSIONS

Bi<sub>2</sub>O<sub>3</sub> thin film with thickness ranging between 0.089 and 0.099 μm and with energy band gaps between 2.50 and 3.60 eV have been successfully deposited in alkaline medium using chemical bath deposition techniques. The EDXRF showed that the films contain bismuth peaks while FTIR spectroscopy showed the bonding peaks and the percentage transmittance, which ranged between 15 and 59% in the far infrared regions.

The deductions from the spectrophotometers showed that average n values ranged from 1.31 to 1.38, k ranged from  $1.63 \times 10^{-3}$  to  $2.22 \times 10^{-3}$ , and  $\sigma_0$  values ranged from  $0.012 \times 10^{14} \text{S}^{-1}$  to  $0.019 \times 10^{14} \text{S}^{-1}$ .

The films were found to have high transmittance in the UV-VIS-NIR regions, in the range between 82 and 100%; hence, they could be effective as thermal control window coatings for cold climates and antireflection coatings.

## REFERENCES

1. Chopra, K.L. and S.R. Das. *Thin Film Solar Cells*. Plenum Press: New York. (1983).
2. Lange, N.A. *Lange's Handbook of Chemistry, 11th ed.* McGraw-Hill Book Co.: New York. (1973).
3. Eze, F.C. and C.E. Okeke. Chemical Bath Deposited Cobalt Sulphide Films; Preparation Effects. *Materials Chemistry and Physics*. 47(1997): 31- 36.
4. Choi J.Y., K.J. Kim, J.B. Yoo and D. Kim. Properties of Cadmium Sulphide Films Deposited by Chemical Bath Deposition with Ultrasonication. *Solar Energy*. 64 (1-3) (1998): 41- 47.
5. Pramanik, P.S., R.N. Bhattacharya and P.K. Basu. A Solution Growth Technique for Deposition of Cobalt Solenoid Thin Films. *Thin Solid Films*. 149(1987): 181.
6. Nair, P.K. and M.T.S. Nair. Solar Assisted Chemical Deposition of Highly Photosensitive CdS Thin Films. *Sol. Ener. Mater.* 15(1987): 431- 440.
7. Nair, P.K. and M.T.S. Nair. Versatile Solar Control Characteristics of Chemically Deposited PbS-CdxS Thin Films. *Semicond. Sci. Technol.* 4(1989): 807- 811.
8. Padam, G.K. and S.U.M. Rao. Preparation and Characterization of Chemically Deposited CuInS<sub>2</sub> Thin Films. *Sol. Ener. Mater.* 13 (1986): 297 - 305.
9. Ndukwe, I.C. Solution Growth, Characterization and Applications of Zinc Sulphide Thin Films. *Sol. Ener. Mater. Sol. Cells*. 40 (1996): 123 - 131.
10. Ortega-Borges, R. and D. Lincot. Chemical Deposition of Cadmium Sulphide Thin Films in the Ammonia Thiourea System. *J. Electrochem. Soc.* 140 (1993): 3464 - 3473.
11. Kaur I., D.K. Pandya and K.L. Chopra. Growth Kinetics and Polymorphism of Chemically Deposited CdS Films. *J. Electrochem. Soc.* 127 (1980): 943 - 948.

12. Nair, P.K., M. Ocampo, A. Fernandez and M.T.S. Nair. Solar Control Characteristics of Chemically Deposited PbS Films for Solar Control Applications. *Sol. Ener. Mater.* 20 (1990): 235 - 239.
13. Nair, P.K., M.T.S. Nair, A. Fernandez and M. Ocampo. Prospects of Chemically Deposited Chalcogenide Thin Films for Solar Control Applications. *J. Phys. D. Appl. Phys.* 22 (1989): 829 - 836.
14. Sabestian, P.J. and H. Hu. Identification of the Impurity Phase in Chemically Deposited CdS Thin Films. *Adv. Mater. Opt. Electron.* 4 (1994): 407 - 412.
15. Pankove, J.I. *Optical Processes in Semiconductors*. Prentice-Hall: New York. (1971).
16. Janai, M., D.D. Alfred, D.C. Booth and B.O. Seraphin. Optical Properties and Structures of Amorphous Silicon Films Prepared by CVD. *Sol. Ener. Mater.* 1 (1979): 11- 27.
17. Theye, M. In: *Optical Properties of Thin Films*. K.L. Chaopra and L.K. Malhotra, eds. Thin Film Technology and Applications. Tata McGraw-Hill, New Delhi, (1985).
18. Ezema, F.I. Solution Growth and Characterization of Binary and Ternary Halide and Chalcogenide Thin Films for Industrial and Solar Energy Applications. Ph.D. Thesis, Department of Physics/Astronomy, University of Nigeria, Nsukka. (2000)
19. Unaogu, A.L. and C.E. Okeke. Characterization of Antimony Doped Tin Oxide Film Prepared by Spray Pyrolysis. *Sol. Energy Mater.* 20, (1990): 29 - 36.
20. Conley, R.T. *Infrared Spectroscopy*. Allyn and Bacon Inc: Boston. (1966).
21. Szafran, Z.N., R.M. Pike, and M.M. Sigh. *Microscale Inorganic Chemistry, A Comprehensive Laboratory Experience*. John Wiley and Sons, Inc: New York. (1991).
22. Ndukwe, I.C. Solution Growth and Characterization of Halide and Chalcogenide Thin Films. Ph.D Thesis. Department of Physics/Astronomy, University of Nigeria: Nsukka. (1993).
23. Ndukwe, I.C. Characterization of Calcium Selenide Thin Films Prepared by Electroless Method. *Nig. Journ. Phys.* 7 (1995): 33 -37.
24. Greenway, D.L. and G. Harbeke. *Optical Properties and Band Structures of Semiconductors*. Pergamon: New York. (1969).

#### **About the Authors:**

**Dr. F.I. Ezema, B.Sc., M.Sc., Ph.D.** serves as a lecturer in the School of General Studies, Natural Sciences Unit and Department of Physics/Astronomy at the University of Nigeria, Nsukka. His research interests are in the areas of thin film deposition, solar energy/solar radiation, and meteorology.

**Professor C.E. Okeke, B.Sc., M.Sc., M.A., Ph.D.** is the Director of the Centre for Energy Research and Development at the University of Nigeria, Nsukka. His research interests include photovoltaics, thin film deposition, and biomass energy conversion.

**Cite As:** Ezema, F.I. and C.E. Okeke. 2003. Chemical Bath Deposition of Bismuth Oxide ( $\text{Bi}_2\text{O}_3$ ) Thin Film and its Applications. *Greenwich Journal of Science and Technology*. 3(2):90-109.

[Return to GJST Home Page](#)